Harla Journals

Harla Journal of Applied Science and Materials
Journal home page:
https://journals.ddu.edu.et/index.php/HJASM

Harla journal
of Applied Science and Materials

Structural, surface, and optical properties of Cerium phosphovanadate prepared by using the solution combustion method

S.J Motloung[1], A.U Yimamu*[2], S.Z Werta[2]

[1]Department of Physics, University of the Free State (QwaQwa Campus), Private Bag X 13, Phuthaditjhaba, 9866, South Africa
[2]Department of Physics, Dire Dawa University, Dire Dawa, Ethiopia
**Corresponding Author*

Abstract

Cerium vanadate ($CeVO_4$), cerium phosphate ($CePO_4$), and cerium phosphovanadate ($CeV_{0.5}P_{0.5}O_4$) powders were synthesized using a solution combustion method. Urea was used as a fuel throughout the experiment. The crystal structure, surface morphology, and elemental composition were characterized by X-ray diffraction (XRD), scanning electron microscopy (SEM), and energy-dispersive X-ray spectroscopy (EDS). The photoluminescence properties of these powders were also studied. XRD results confirmed the formation of $CeVO_4$, $CePO_4$ and $CeV_{0.5}P_{0.5}O_4$ single structures. Furthermore, the XRD results indicated that $CeV_{0.5}P_{0.5}O_4$ is an admixture of $CeVO_4$ and $CePO_4$. The estimated crystallite sizes from the Scherrer formula were 12, 16, and 14 nm for $CeVO_4$ $CePO_4$ and $CeV_{0.5}P_{0.5}O_4$, respectively. SEM images of $CePO_4$ and $CeV_{0.5}P_{0.5}O_4$ indicated that the samples were agglomerated and did not possess any clear shapes, with the particles of $CeVO_4$ being less agglomerated and having clearer mixed shapes. The EDS spectra showed the presence of all major elements. The photoluminescence emission results of all the powdered samples showed a large peak at 467nm due to 2F→2D transitions of Ce^{3+} ions. $CePO_4$ displayed the highest emission peak.

Key words/Phrases: Cerium vanadate; optic; photoluminescence; X-ray diffraction

1. Introduction

Recently, there has been much research in rare earth phosphate nanoparticles' production and characterization because of their properties related to photoluminescence and photocatalysis. Among these rare earth phosphates, $CePO_4$ nanomaterials have drawn more and more interest since its $CePO_4$ bulk crystal material already demonstrates various applications [1]. $CePO_4$ can be used in luminescent green light, which is produced very effectively by luminescent lights. The two polymorphs of $CePO_4$ are hexagonal and monoclinic in nature [2].

**Corresponding author: A.U Yimamu; email: ahed.dilla@gmail.com; Cell phone: +251930509797*

Received: July 2023; Received in revised form: September 2023; Accepted: December 2023

Lima *et al.* [3] reported that monoclinic $CePO_4$ nanoparticles have an application in sunscreen materials, acting as a UV filter with excellent morphological characteristics, desirable UV absorption features, low toxicity, and ideal particle size for sunscreen formulations $CePO_4$ is a cerium compound that exhibits great fluorescence in the visible spectrum and substantial absorption in the ultraviolet spectrum. The f–d electron transitions of Ce^{3+} ions are responsible for these visual characteristics [4]. The luminescence characteristics of phosphors depend largely on the host materials; hence, choosing a proper host is very important [5]. Low phonon energy cerium phosphate in monazite form prevents undesired nonradiative energy loss through multi-phonon relaxation [6]. $CePO_4$ is a lanthanide phosphate and can be used as a catalyst for the oxidative dehydrogenation of isobutane, amination of 1-octanol, vapor-phase Oalkylation of phenol, dehydration reaction of 2-propanol and selective catalytic reduction of NO with NH_3 [7].

Rare earth vanadates, on the other hand, are used in various applications such as in fuel cells, luminescence, and photocatalysis due to their 4f–5d and 4f–4f electronic transitions [8]. $CeVO_4$ is a rare earth vanadate that has been used in a variety of disciplines because of its optical, electrical, magnetic, and catalytical qualities [9]. The deficiency of UV light severely obstructs the photocatalysis process from having any practical uses. In an effort to increase the efficiency of sunlight's usage, scientists and researchers are now concentrating on certain visible-light-driven photocatalysts. Cerium vanadate's ($CeVO_4$) broad spectrum of light absorption, electronic band structure, and crystallinity make it a good photocatalyst [10]. $CeVO_4$ nanomaterials are chemically, photothermally, and photochemically stable, easy to synthesize, and can simultaneously absorb broad near-infrared photons to achieve up-conversion luminescence [11]. As an important semiconductor, $CeVO_4$ has been investigated in catalysis and gas sensor fields. Until now, various $CeVO_4$ nanostructures have been prepared, including nanorods, nanoplates, nanobelts, and microspheres [12].

In this study, $CePO_4$, $CeVO_4$, and $CeV_{0.5}P_{0.5}O_4$ nanoparticles were synthesized using a solution combustion method using urea as a fuel. The method was chosen because of its rapidness, cost-effectiveness, and simplicity. The structure, morphology, elemental composition and luminescence properties of the synthesized particles were investigated. To the best of our knowledge, there are no reports on the synthesis of cerium phosphovanadate by the solution combustion process. The ultimate goal of this work is to investigate the effect of the synthesis method on the structural, morphological, and photoluminescent properties of $CeV_{0.5}P_{0.5}O_4$ synthesized by the solution combustion method.

2. Experimental Materials

Ammonium metavanadate (NH_4VO_3), cerium (iii) nitrate hexahydrate (Ce(NO3)3.6H2O), urea (CH_4N_2O) and ammonium dihydrogen phosphate (NH4H2PO4) were used as starting materials. All the raw materials used were of analytical reagent grade and were used without further purification.

2.1. $CePO_4$ preparation

$CePO_4$ powder was synthesized using a solution combustion method using urea as a fuel. Stoichiometric amounts of $Ce(NO_3)_{3.6}H_2O$, urea, and $NH_4H_2PO_4$ were mixed in a

glass beaker and dissolved in 10 mL of de-ionized water. The contents of the beaker were stirred and heated at a constant temperature of 80°C for 45 min on an electric magnetic hot plate. The solution was transferred into a crucible, which was placed in a muffle furnace preheated to 600˚C ± 10˚C. The solution boiled, and the water evaporated within 10 min. The resulting powder was removed from the furnace and cooled to room temperature. Finally, the powder was ground using a pestle and mortar, and it was ready for characterization. A similar procedure was followed for the synthesis of $CeVO_4$ and $CeV_{0.5}P_{0.5}O_4$, respectively.

2.2. Characterization

A Bruker AXS D8 advance diffractometer (XRD) was used to determine the structure of the samples. The radiation source was Cu-Kα (λ = 1.5406Å). The morphology and elemental composition were obtained using SEM. The photoluminescence measurements were recorded using the Hitachi F700 fluorescence spectrophotometer.

3. Results and discussion

3.1. X-ray diffraction

The XRD patterns of $CePO_4$, $CeVO_4$, and $CeV_{0.5}P_{0.5}O_4$ are displayed in Figure 1. The diffraction peaks of $CeVO_4$ are consistent with the peaks in JCPDS file no. 12-0757, which corresponds to a tetragonal structure of cerium vanadium oxide. The XRD pattern does exhibit an impurity peak at 28° (2 theta), and this can be associated with CeO_2 [13]. Furthermore, the peaks of $CeVO_4$ are slightly shifted to the right, possibly due to lattice strain in the crystal. The diffraction peaks of $CePO_4$ correspond to the hexagonal structure of cerium phosphate referenced in JCPDS file no. 75-1880. No impurity peaks can be observed for the $CePO_4$ powder. The XRD pattern of $CeV_{0.5}P_{0.5}O_4$ comprises the peaks from both $CeVO_4$ and $CePO_4$. This suggests that $CeV_{0.5}P_{0.5}O_4$ is an admixture of $CeVO_4$ and $CePO_4$. In general, the diffraction peaks of the prepared powder samples are broad, which suggests that the powder has a small crystallite size.

The Scherrer formula was used to determine the crystallite size D using Equation 1

$$D=0.94\lambda/\beta\cos\theta \quad (1)$$

where θ is the Bragg diffraction angle, and β is the peak's full width at half maximum (FWHM) in radians. The estimated sizes from the Scherrer formula were 12, 16, and 14 nm for $CeVO_4$, $CeV_{0.5}P_{0.5}O_4$, and $CePO_4$, respectively.

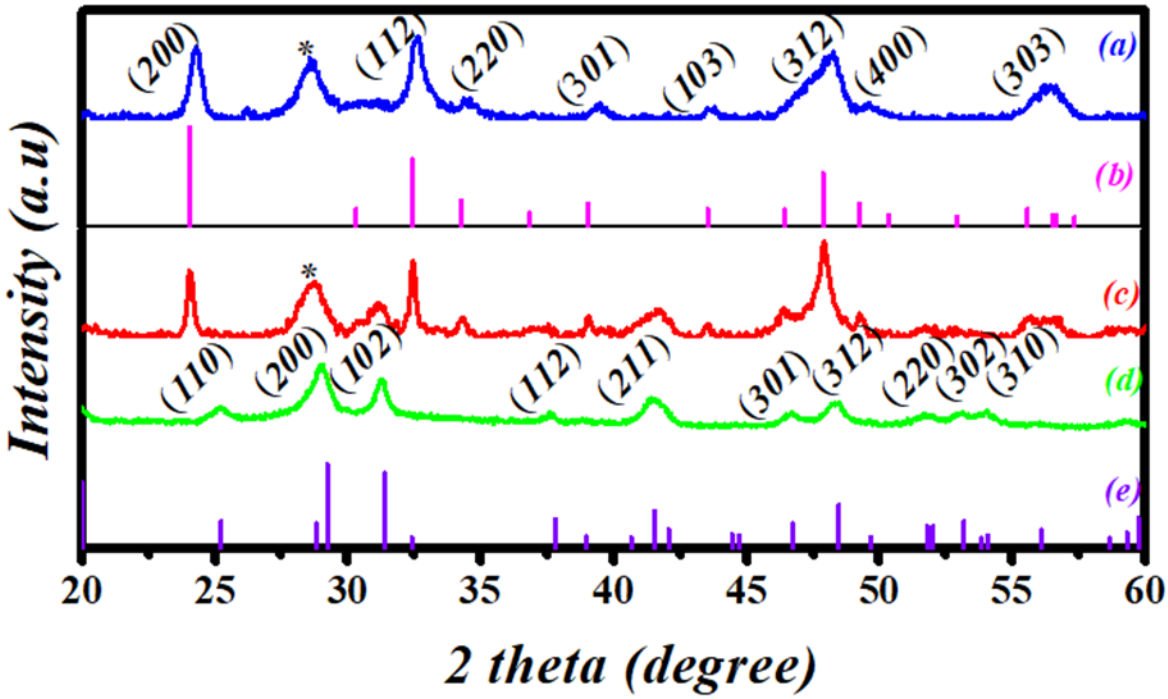

Figure 1: XRD patterns of (a) $CeVO_4$, (b) JCPDS no: 12-0757, (c) CeV0.5P0.5O0.4 and (d) $CePO_4$, and (e) JCPDS no: 75-1880.

3.2. **Scanning Electron Spectroscopy**

The surface morphology of the prepared powders was investigated using SEM. Figure 2 displays SEM images of (a) $CePO_4$, (b) $CeV_{0.5}P_{0.5}O_4$, and (c) $CeVO_4$. The SEM images of $CePO_4$ and $CeV_{0.5}P_{0.5}O_4$ indicate that the samples are agglomerated and have no clear shapes. But, there are also traces of small particles distributed on the agglomerates. On the other hand, the particles of $CeVO_4$ are less agglomerated and have clear shapes. They mainly possess spherical shapes and a few other mixed shapes. The grain size of $CeVO_4$ has different shapes and arrangements, as shown in Figure 2 c.

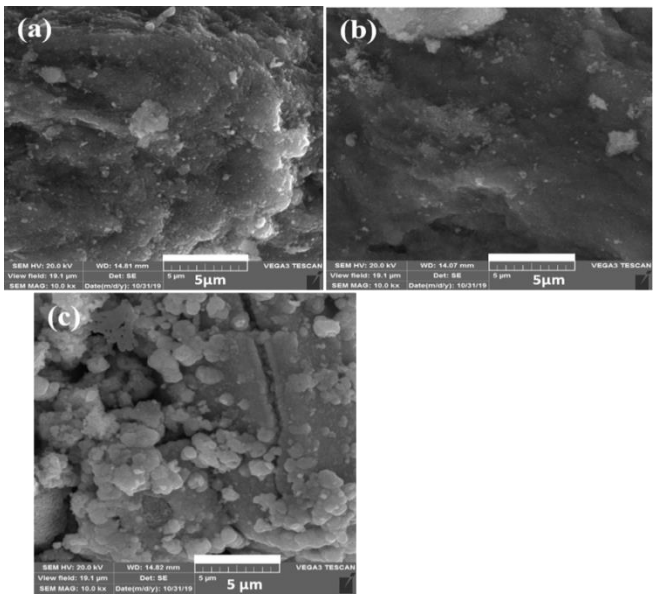

Figure 1: SEM images of (a) $CePO_4$, (b) $CeV_{0.5}P_{0.5}O_4$ and (c) $CeVO_4$

3.3. Energy-dispersive X-ray spectroscopy

The elemental composition of the prepared powders was determined by energy-dispersive X-ray spectroscopy (EDS). The recorded results of EDS are displayed in Figure 3. The spectra show the presence of all major elements. The composition of Figure 3 (a) confirms the formation of $CePO_4$. The prepared $CePO_4$ consists of 67.2 wt% Ce, 20.2 wt% O and 12.2 wt% P. The elemental composition of Figure 3 (c) confirms the formation of $CeVO_4$. The prepared $CeVO_4$ powder consists of 64.5 wt% Ce, 20.5 wt% O and 15 wt% V. The elemental composition of Figure 3 (b) confirms the formation of $CeV_{0.5}P_{0.5}O_4$. The prepared $CeV_{0.5}P_{0.5}O_4$ comprises 64.3 wt% Ce, 20.7 wt% O, 8.9 wt% P and 6.1 wt% V. The presence of carbon elements in Figure 3 (a), (b), and (c) is due to the carbon tape used to mount the samples

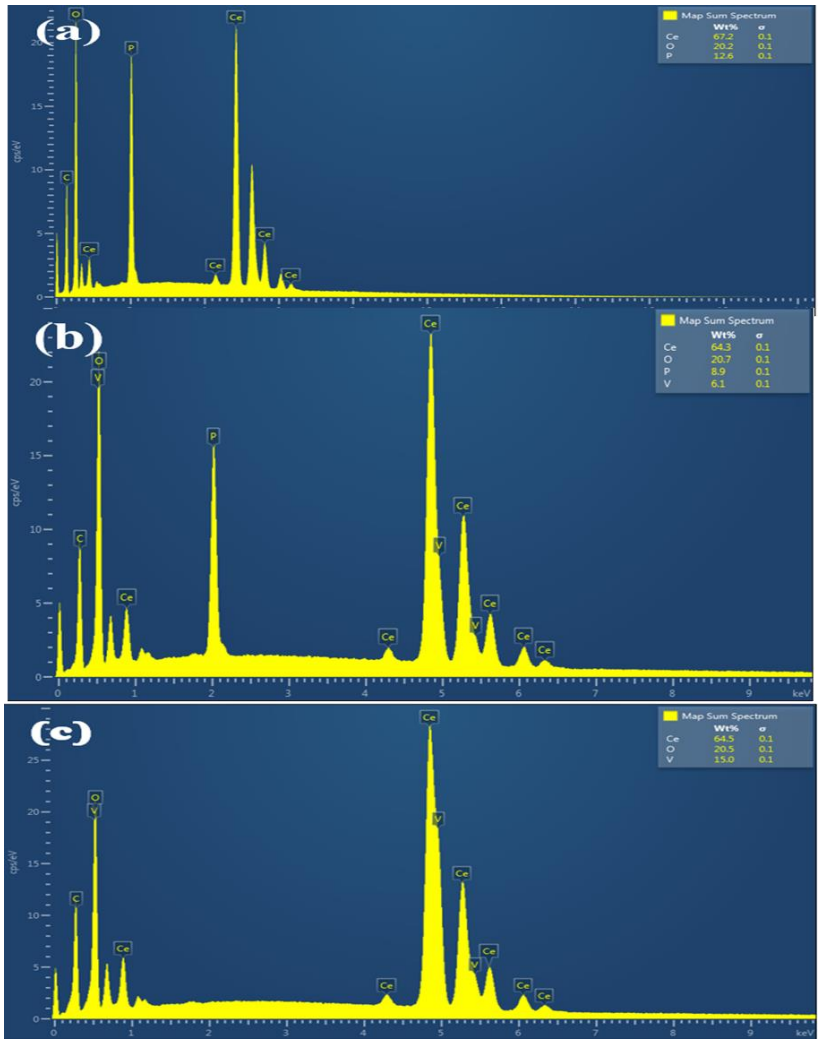

Figure 3: EDS spectra of (a) $CePO_4$, (b) $CeV_{0.5}P_{0.5}O_4$ and (c) $CeVO_4$

3.4. Photoluminescence spectroscopy

Figure 4(a) displays the excitation spectra of $CePO_4$, $CeV_{0.5}P_{0.5}O_4$, and $CeVO_4$ powders. These spectra were recorded while monitoring the emission wavelength of 467 nm. All the samples exhibited a broad band between 200 nm and 300 nm. This broadband can be attributed to charge transfer from oxygen ligands to the central vanadium and phosphorus atoms. The emission spectra of $CePO_4$, $CeV_{0.5}P_{0.5}O_4$, and

$CeVO_4$ recorded by monitoring the excitation wavelength at 210 nm are presented in Figure 4(b). The spectra show an emission peak at 467 nm protruding from a broad band extending from 400 nm to 650 nm. Palma-Ramirez *et al.* [14] ascribed this emission peak to 2F→2D transitions of Ce^{3+} ions.

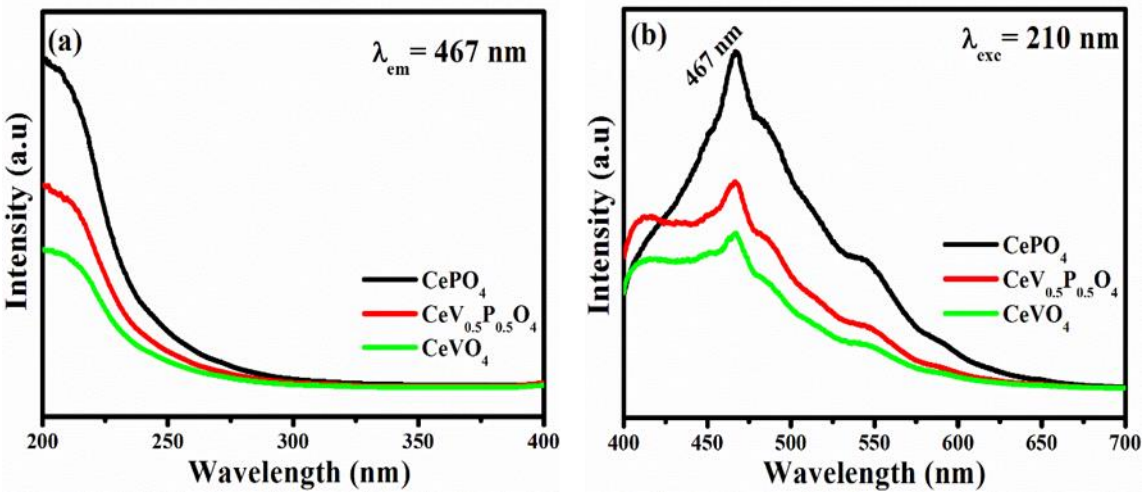

Figure 2: The photoluminescence spectra of $CePO_4$, $CeVO_4$ and $CeV_{0.5}P_{0.5}O_4$

4. Conclusion

The $CePO_4$, $CeVO_4$, and $CeV_{0.5}P_{0.5}O_4$ nanoparticles were successfully synthesized using urea as a fuel using a solution combustion method. The XRD results confirmed that the prepared powders of $CePO_4$ and $CeVO_4$ possessed hexagonal and tetragonal structures, respectively. The XRD results also indicated that $CeV_{0.5}P_{0.5}O_4$ is an admixture of $CeVO_4$ and $CePO_4$. SEM images of $CePO_4$ and $CeV_{0.5}P_{0.5}O_4$ indicated that the samples were agglomerated and had no precise shapes. SEM also showed that the particles of $CeVO_4$ were slightly agglomerated and possessed mixed shapes. The elemental composition of the synthesized powders confirmed the formation of $CePO_4$, $CeVO_4$, and $CeV_{0.5}P_{0.5}O_4$. Photoluminescence spectroscopy results indicated that all the samples absorbed wavelengths between 200nm and 300nm in the ultraviolet region of the electromagnetic spectrum. The photoluminescence spectroscopy spectra also indicated that the samples emitted wavelengths between 400nm and 650nm in the visible light region of the electromagnetic spectrum.

5. Acknowledgments

The author of this report would like to thank the South African National Research Foundation for the financial assistance of the University of the Free State QwaQwa campus for the opportunity to study and Dire Dawa University, Physics department.

6. References

[1] Z. Zhu, K Zhang, H. Zhao, J. Zhu, UV-light driven photocatalytic performance of hydrothermally-synthesized hexagonal $CePO_4$ nanorods, Solid State Sciences 72 (2017) 28-32.

[2] M.G. Ma, J.F. Zhuc, S.W. Caod, F. Chend, R.C. Suna, Hydrothermal synthesis of relatively uniform $CePO_4$@LaPO4 one-dimensional nanostructures with highly improved luminescence, Journal of Alloys and Compounds 492 (2010) 559–563.

[3] J.F. de Lima, O.A. Serra, Cerium phosphate nanoparticles with low photocatalytic activity for UV light absorption application in photoprotection, Dyes Pigm 97 (2013) 291-296.

[4] A.S. Dezfuli, M.R. Ganjali, P. Norouzi, Facile sonochemical synthesis and morphology control of CePO4 nanostructures via an oriented attachment mechanism: Application as luminescent probe for selective sensing of Pb2+ ion in aqueous solution, Materials Science and Engineering C 42 (2014) 774–781.

[5] G.S.R. Raju, J.S. Yu, J.Y. Park, H.C. Jung, B.K. Moon, Photoluminescence and cathodoluminescence properties of nanocrystalline Ca2Gd8Si6O26:Sm3+ phosphors, J. Am. Ceram. Soc. 95 (2012) 238–242.

[6] S. Sisira, D. Alexander, K. Thomas, P.R. Biju, N.V. Unnikrishnan, C. Joseph, Effect of annealing temperature on the luminescence of Ce1-xPO4: Tbx3+ nanocrystals: a novel theoretical model and experimental verification, J. Mater. Sci. 53 (2018) 1380–1394.

[7] H. Liu, Z. Ma, Rh2O3/monoclinic $CePO_4$ composite catalysts for N2O decomposition and CO oxidation, Chinese Journal of Chemical Engineering 26 (2018) 109–115.

[8] L. Fengzhen, S. Xin, Y. Yibin, Z. Limin, S. Zhuwei, L. Xuehua, M. Xianhua, Shape controlled synthesis and tribiological properties of $CeVO_4$ nanoparticles as lubricating additive, J. Rare Earths 29 (2011) 688–691.

[9] S. Mishra, M. Priyadarshinee, A.K. Debnath, K.P. Muthe, B.C. Mallick, N. Das P. Parhi, Rapid microwave assisted hydrothermal synthesis cerium vanadate nanoparticle and its photocatalytic and antibacterial studies, Journal of Physics and Chemistry of Solids 137 (2020) 109-211.

[10] L. Yao, E. Guo, K. Sun, Q. Lu, Q. Wang, Formation of one-dimensional $CeVO_4$ nanobelts as an enhanced photoelectrocatalyst and density functional study, Materials Letters 231 (2018) 11–15.

[11] Z. Chen, H. Jia, K. Sharafudeen, W. Dai, Y. Liu, G. Dong, J. Qiu, Up-conversion luminescence from single vanadate through blackbody radiation harvesting broadband near-infrared photons for photovoltaic cells, Journal of Alloys and Compounds 663 (2016) 204-210.

[12] M. Wang, X. Hu, Z. Zhan, T. Sun, Y. Tang, Facile fabrication of $CeVO_4$ hierarchical hollow microspheres with enhanced photocatalytic activity, Materials Letters 253 (2019) 259–262.

[13] G. Liu, L. Chen, X. Duan, D. Liang, Synthesis and characterization of Sm3+-doped CeO_2 powders, Trans. Nonferrous. Met. Soc. China 18 (2008) 897-903.

[14] D. Palma-Ramirez, M.A. Dominguez-Crespo, A.M. Torres-Huerta, V.A. Escobar-Barrios, H. Dorantes-Rosales, H. Willcock, Polymer 142 (2018) 356-374